SHORT COMMUNICATION

FUNCTIONALISATION OF MESOPOROUS SILICA NANOPARTICLES WITH A CELL-PENETRATING PEPTIDE AS A TOOL FOR THE SPECIFIC TARGETING OF MAMMALIAN SPERM *IN VITRO*

Natalia Barkalina, MD, MSc[1] (natalia.barkalina@obs-gyn.ox.ac.uk),
Celine Jones[1] (celine.jones@obs-gyn.ox.ac.uk),
Helen Townley, PhD[1,2] (helen.townley@eng.ox.ac.uk)
Kevin Coward, PhD[1] (kevin.coward@obs-gyn.ox.ac.uk).

[1]*Nuffield Department of Obstetrics and Gynaecology, University of Oxford, Level 3, Women's Centre, John Radcliffe Hospital, Headington, Oxford, OX3 9DU, UK;*
[2]*Department of Engineering Science, University of Oxford, Parks Road, Oxford, OX1 3PJ*

Corresponding author (address for reprints): Kevin Coward, PhD, Nuffield Department of Obstetrics and Gynaecology, Level 3, Women's Centre, John Radcliffe Hospital, Headington, Oxford, OX3 9DU, United Kingdom (Telephone: +441865 782878; E-mail: kevin.coward@obs-gyn.ox.ac.uk).

STRUCTURED ABSTRACT (120 WORDS ALLOWED; 131 WORDS NOW)

Aims: This study aimed to investigate the effects of actively targeting spherical mesoporous silica nanoparticles (MSNPs) with hexagonal pore symmetry towards mammalian sperm with a specific cell-penetrating peptide (C105Y) with subsequent analysis of binding rates and nano-safety profiles. **Materials and methods:** Boar sperm were exposed *in vitro* to MSNPs, functionalized with C105Y via covalent absorption, or free C105Y, in a series of increasing doses for up to 2 hours, followed by sperm motility evaluation, and analysis of kinematic parameters, acrosome morphology, MSNP-sperm association rates, and levels of cell fluorescence. **Results:** C105Y-functionalised MSNPs preserved their biocompatibility with sperm, and exhibited an approximately 4-fold increase in affinity towards gametes, compared to unmodified MSNPs, during the early stages of incubation. **Conclusion:** Our findings support the application of MSNPs and active targeting to sperm as valuable tools for reproductive biology.

Keywords: Nanoparticles; mesoporous silica; sperm; cell-penetrating peptides; functionalisation; delivery.

1. INTRODUCTION

Nanotechnology is a rapidly expanding discipline with multiple applications for biological research and clinical medicine, allowing the design and engineering of highly sensitive and selective small-scale (<100nm) platforms for the targeted detection and experimental treatment of a variety of pathological conditions [1]. In recent years, there has been growing interest in the use of nanomaterials for reproductive biology, particularly for the delivery of various molecular cargoes into gametes as a way to improve the efficacy of many research techniques, involving the internalisation of compounds into sperm and oocytes, and promote their wider use [2]. These techniques include, but are not limited to, gene transfer into reproductive tissues [3, 4], sperm-mediated gene transfer (SMGT) [5], an investigative tool based on the physiological property of sperm to bind, incorporate and deliver exogenous DNA into the oocyte at the time of fertilisation resulting in the production of transgenic/mosaic embryos, and the sorting of sperm into sub-populations driven by the detection of a specific intracellular marker, for example sex sorting [6]. Although these experimental techniques have been extensively studied over the last few decades, their efficacy remains sub-optimal [3, 6-8], and their relative application is thus compromised.

The challenge facing biological delivery methods in reproductive biology is generally attributed to the highly specialised structure and function of reproductive tissues and gametes, resulting in high levels of physiological resistance towards the uptake of exogenous compounds [9]. Such factors readily justify the need for the

development of new delivery tools that are safe but can also be customised and targeted to these unique cell populations in order to internalise discrete molecular cargoes. There is steadily growing evidence that the essential processes of reproduction, including oocyte maturation, sperm membrane remodelling and the acquisition of fertilisation capacity, are mediated by natural cell-secreted organic micro- and nanoparticles referred to as exosomes and microvesicles [10-12]. Consequently, the application of similar engineered small-scale tools to target and manipulate the sophisticated processes underlying key phases of reproductive biology appears particularly logical.

Recent studies have provided increasing evidence to support the use of nanomaterials for intra-gamete delivery. In the case of SMGT, loading exogenous DNA onto nanoparticles has been demonstrated to significantly increase the efficacy of molecular construct internalisation into sperm [13-15]. Additionally, the versatility and large loading capacity of nanomaterials permit users to load nanocarriers with a wide range of non-nucleic acid compounds, such as peptides/proteins [16], fluorescent probes [17], or recognition sequences for specific intracellular markers [6], and subsequently deliver this cargo successfully into sperm for the purposes of bioimaging, cell sorting or subsequent transfer into the oocyte. However, the range of nanomaterials with proven reproductive safety remains limited, and despite the successful delivery of compounds, such as the internalisation of exogenous DNA into sperm, many studies fail to demonstrate successful integration into early embryos following fertilisation [13, 14].

Although nanoparticle-mediated delivery into gametes appears technically straightforward and practically beneficial, its efficacy is lower than that evident with somatic cells. Most nanomaterials applied to gametes have been reported to primarily sequestrate onto the cell surface or inside the plasma membrane, with a relatively small proportion of nanocarriers reaching the cytoplasmic compartment [13, 17-21]. Despite observations that such profiles of association do not affect the transfer of molecular cargo from the nanocarrier into target cells [13], the development of new strategies to facilitate the uptake of nanomaterials by gametes is pre-exquisite for the wider introduction of nanoparticle-mediated delivery into reproductive biology for both research and potential therapeutic application.

Functionalisation of the surface of nanomaterials with specific affinity ligands, including antibodies, aptamers, proteins, peptides, and small molecules, which selectively bind with specific surface receptors in a target cell population, represents a common approach for improving the accuracy of both cargo transport and uptake, and minimising off-target interaction [22]. Although active targeting is widely used in the design of nanomaterials for systemic applications, its benefits for the *in vitro* delivery of cargo into gametes has not been extensively studied. Successful active targeting in gametes requires careful selection of affinity ligands which would not interact with gamete surface receptors involved in fertilisation and thus result in their premature activation or inhibition. This requirement could limit the use of traditional functionalization tools, such as antibodies, and require the use of alternative targeting

moieties, among which cell-penetrating peptides represent a particularly interesting option.

Cell-penetrating peptides (CPPs) are a specific class of short cationic/amphipathic peptides (<30 amino acids) with a remarkable ability to translocate across the plasma membrane in a receptor- and energy-independent manner, and are able to transport a considerably larger molecular cargo into cells [23, 24]. CPPs represent a relatively novel class of functionalisation agents for nanomaterials, with the first studies into the effects of CPP coating upon nanomaterial uptake commencing around fifteen years ago [25]. Nevertheless, over the last 10 years, CPP-functionalised nanomaterials have been consistently shown to exhibit improved cellular uptake in a variety of cell types, and are currently being proposed as a promising alternative to more conventional active targeting moieties [26, 27]

Recently, a 17-amino acid synthetic poly-cationic peptide known as C105Y (CSIPPEVKFNKPFVYLI) [28], has been characterised as displaying high affinity towards mammalian sperm, together with encouraging safety profiles and predominant distribution in the non-acrosomal portion of the sperm head and mid-piece [29]. Low toxicity and accumulation in the sperm head, but, at the same time, not in the regions involved in the earliest stages of fertilisation, render C105Y an attractive candidate for the surface functionalisation of nanocarriers for intra-sperm delivery. In a recent study, we demonstrated the biocompatibility of spherical mesoporous silica nanoparticles (MSNPs) exhibiting hexagonal pore symmetry and

various surface chemical modifications with mammalian sperm following *in vitro* exposure, and their ability to bind strongly with the plasma membrane of approximately 20% of sperm in a typical sample [21].

Here, we present the outcomes of an extension study, demonstrating that the functionalization of MSNPs with C105Y further increases the binding rate of particles with boar sperm following *in vitro* exposure, with satisfactory safety profiles. Our findings, therefore, provide a rationale for the surface functionalization of nanoparticles with gamete-specific affinities in order to improve their specificity for applications in reproductive biology.

2. METHODS

2.1. SYNTHESIS OF MSNPS

MSNPs were synthesised in a surfactant-templated base-catalysed sol-gel reaction, as described previously [21, 30]. In brief, 100mg of hexadecyltrimethylammonium bromide (CTAB, >99%, Sigma-Aldrich, UK) was dissolved in a mixture of 48ml double distilled water (DDW) and 0.35ml of 2M sodium hydroxide (anhydrous NaOH, ≥98%, Sigma-Aldrich, UK) in a round-bottomed flask. The solution was heated in a silicone oil bath to 80°C with magnetic stirring. After the temperature had stabilised, 0.5ml of tetraethyl orthosilicate (TEOS, 98%, Sigma-Aldrich, UK) was added to the reaction. After 15 minutes, 0.127ml of 3-(trihydroxysilyl)propyl methylphosphonate (3-THPMP, monosodium salt, 42 wt.% solution in water, Sigma-Aldrich, UK) was added, and reaction was stirred for 2 hrs at 80°C. The solution was

then cooled to room temperature (RT), and MSNPs were recovered and washed with methanol (≥99.8%, Rathburn Chemicals, UK) by centrifugation. Particles were redispersed in a mixture of 40ml of methanol and 2ml of 12.1M hydrochloric acid (HCL; 37.2 wt.% solution in water, 12.1M, Sigma-Aldrich, UK), and refluxed for 24 hrs at 80°C with magnetic stirring to remove CTAB. After refluxing, MSNPs were washed in absolute ethanol (≥99.8%, Riedel-de Haën, Germany), and vacuum dried overnight.

2.2. Functionalisation of MSNPs with C105Y

The surface of synthesised MSNPs was functionalised with (3-aminopropyl)triethoxysilane (APTES, ≥98%, Sigma-Aldrich) to provide amine groups for covalent cross-linking with carboxyl groups of the C105Y-TMR fluorescent peptide (tetramethylrhodamine-CSIPPEVKFNKPFVYLI-CONH2, Covalab, France). For surface coating, MSNPs were redispersed in DDW to a concentration of 10mg/ml, and APTES was added to 5% by volume. The reaction was stirred magnetically for 1 hour at RT. Coated particles were recovered, washed in sterile DDW by centrifugation, and vacuum dried overnight.

APTES-coated MSNPs were functionalised with C105Y-TMR via the cross-linking of amine groups on the functionalised surface of MSNPs with carboxyl groups of the peptide using 1-ethyl-3-[3-dimethylaminopropyl]carbodiimide hydrochloride coupling agent (EDC, Fisher Scientific, UK). In brief, 2mg of APTES-functionalised MSNPs were redispersed in 200µl of 0.1M 2-[n-morpholino]ethane sulfonic acid-buffered saline (MES-buffered saline, Fisher

Scientific, UK) and mixed with 200µl of C105Y-TMR (2mM in 10% acetic acid, Sigma-Alrdich, UK). The resulting suspension was diluted with 1500µl of 0.1M MES buffer, and 100µl of EDC (10mg/ml in DDW) was immediately added to the reaction. The reaction was incubated for 2 hours at RT on a shaker plate. C105Y-TMR-functionalised MSNPs were recovered through centrifugation, and redispersed in phosphate-buffered saline (PBS, Oxoid, UK).

2.3. Characterisation of MSNPs

Detailed characterisation of synthesised MSNPs prior to cargo loading using a combination of conventional analytical chemistry tools was carried out in the previous study [21]. In particular, the physical size and shape of synthesised MSNPs were evaluated by transmission electron microscopy (TEM; JEOL JEM-2010, JEOL Ltd., Japan) and scanning electron microscopy (SEM; JEOL JSM-840F, JEOL Ltd., Japan), respectively. For this set of experiments, unmodified and C105Y-functionalised MSNPs were characterised for ζ potential in incubation medium (Beltsville Thawing Solution, BTS, pH 7.33) using electrophoretic light scattering (Zetasizer Nano ZS, Malvern Instruments, UK), and hydrodynamic size was determined in phosphate-based saline (Dulbecco's PBS, Sigma-Aldrich UK, pH 7.4) by nanoparticle-tracking analysis (Nanosight LM10, Malvern Instruments, UK). Binding of C105Y-TMR with MSNPs was confirmed by the spectrophotometric measurement of peptide concentration in solution before and after the reaction (BiophotometerPlus, Eppendorf, UK).

2.4. Semen preparation and exposure of sperm to C105Y-functionalised MSNPs

Preparation and application of MSNPs to mammalian sperm was carried out in a manner similar to that described previously [21]. In brief, boar sperm, a common model for human sperm in pilot reproductive biology experiments, were obtained from a licensed pig breeding company (JSR Genetics, UK) in a commercial extender at 17ºC. Sperm was activated by incubation for 15 minutes at 35°C, and concentration determined in a Bürker-Turk haemocytometer at 200x magnification using a positive contrast phase objective (Nikon UK Ltd.). Following activation, 1ml aliquots were withdrawn from each sample, centrifuged at 500g for 10 minutes, washed from the extender with PBS, and resuspended in BTS (37g dextrose hydrate, 6g sodium citrate dehydrate, 1.25g sodium bicarbonate, 1.25g disodium ethylenediamine tetraacetate, 0.75g potassium chloride, 1000ml DDW; pH 7.33 [31]). Sperm were then treated with C105Y-functionalised MSNPs at a ratio of 10µg, 15µg and 30µg of particles per 10^7 sperm, or free C105Y (0.02mM in 10% acetic acid) in a quantity equivalent to that adsorbed on the MSNPs, or BTS (controls). Incubation was carried out for up to 2 hrs at 37ºC under a low-oxygen atmosphere, in accordance with our previous findings indicating that stable binding of MSNPs to sperm can be observed after as little as 2 hrs of *in vitro* exposure [21]. Sperm motility, viability and acrosome morphology were assessed after 2 hrs of incubation. Association rates between sperm and C105Y-functionalised MSNPs were determined after 1 and 2 hrs. Levels of cell fluorescence in sperm exposed to C105Y-functionalised MSNPs, and equivalent doses of free C105Y, were also

evaluated after 1 and 2 hrs. Each experiment was replicated a minimum of three times using samples obtained from different animals.

2.4.1. SPERM MOTILITY AND MORPHOLOGY ASSESSMENT

Assessment of total and progressive motility was performed using a computer-assisted sperm analysis system (CASA; HTM-Ceros v.12.3, Hamilton Thorne, MA, USA). Analysed parameters included total motility (%), progressive motility (%), proportions of sperm within the standard 'rapid', 'medium', 'slow' and 'static' categories (%), smoothed path velocity (VAP, μm/sec), straight line velocity (VSL, μm/sec), track velocity (VCL, μm/sec), amplitude of lateral head displacement (ALH, μm), and beat cross frequency (BCF, Hz). For CASA, samples were loaded into a 20μm-deep Leja counting chamber, and equilibrated on a warm stage (37°C) for 2 minutes. Images were acquired at 100x magnification using a negative contrast phase objective (Nikon UK Ltd.). A minimum of 10 fields, containing at least 400 sperm, were evaluated in each sample.

For morphology assessment, we focused specifically upon acrosome morphology as a relatively straightforward tool to evaluate the acute effects of sub-optimal environment upon boar sperm morphology [32]. Acrosome morphology was evaluated in unstained 10μl drops, fixed with 4.5% phosphate buffered formalin solution (Sigma-Aldrich, UK). A minimum of 100 sperm per sample were assessed for the integrity of an acrosomal apical ridge at 1000x magnification using a positive contrast phase oil-immersion objective (Leica Microsystems UK Ltd.), and

classified into 4 categories: normal apical ridge (NAR), damaged apical ridge (DAR), missing apical ridge (MAR), and loose acrosomal cap (LAC).

2.4.2. Determination of the association rate between C105Y-TMR-functionalised MSNPs and sperm fluorescence levels

Quantification of the number of sperm associated with C105Y-functionalised MSNPs was carried out in a manner similar to that reported previously [21]. In brief, samples were fixed with 10% formalin solution (Sigma-Aldrich, UK) after 1 and 2 hrs of incubation, and then washed from the fixative and unbound MSNPs in PBS via centrifugation. Sperm were transferred to poly-L-lysine coated slides, incubated in a humidifying chamber for 30 minutes at RT, washed twice in PBS, and mounted with glycerol-based medium (Vectashield H-1000, Vector Laboratories, UK). Slides were then examined at 400x magnification under a fluorescent microscope with 540-588nm (red) excitation wavelength filters (Nikon UK Ltd.). Detailed imaging was performed at 600x magnification with an oil-immersion objective under a confocal laser microscope with a 559nm (red) excitation line (Olympus UK Ltd.). Acquired images were processed with Fiji/ImageJ 1.47i (National Institute of Health, USA). The number of sperm associated with MSNPs was counted in approximately 200 cells per sample. Corrected cell fluorescence levels were calculated by subtracting the intensity of background fluorescence from the total pixel intensity value (red channel) in the projection of approximately 100 individual morphologically intact sperm per experimental condition [33], and expressed in arbitrary units (AU) per $1\mu m^2$ of sperm surface.

2.5. STATISTICAL ANALYSIS

Data are presented as the mean±standard error of the mean (SEM), unless specified otherwise. All variables were checked for normality using the Kolmogorov-Smirnoff test and subjected to log-linear or arcsine-square root transformation where appropriate. Data were analysed using a generalized linear mixed model (GLMM) with post-hoc sequential Bonferroni adjustment and type of treatment (control/C105Y-functionalised MSNPs/free C105Y), dose ratio, and time, as fixed factors, and with ejaculate as a random factor. For a detailed investigation of the effects of dose and the duration of exposure to C105Y-functionalised MSNPs, or free C105Y, upon individual sperm, GLMM was followed by logistic regression analysis of categorical data (total/progressive motility, proportion of sperm with NAR, and association rate between sperm and C105Y-functionalised MSNPs), controlled for inter-sample variability. Control samples were used as a reference category for the assessment of motility and morphology parameters; association rates between sperm and C105Y-functionalised MSNPs were compared with retrospective data for unmodified MSNPs [21]. Differences were considered significant at $p \leq 0.05$. Statistical analysis was performed using IBM SPSS Statistics v20.0 (IBM, Armonk, NY, USA). Representative figures were constructed in GraphPad Prism v6.0 (GraphPad Software, La Jolla, CA, USA).

3. RESULTS

3.1. CHARACTERISATION OF MSNPS

Characterisation data of unmodified MSNPs was reported in our previous publication [21]. In brief, synthesised MSNPs were slightly non-spherical with elongation in the direction of the pore channels, and with ordered nanometre-sized pores displaying hexagonal symmetry when aligned with the beam (Figure 1, reproduced from [21]). Prior to functionalization with C105Y, MSNPs had an average physical diameter of ~138nm with ~2nm-sized pores.

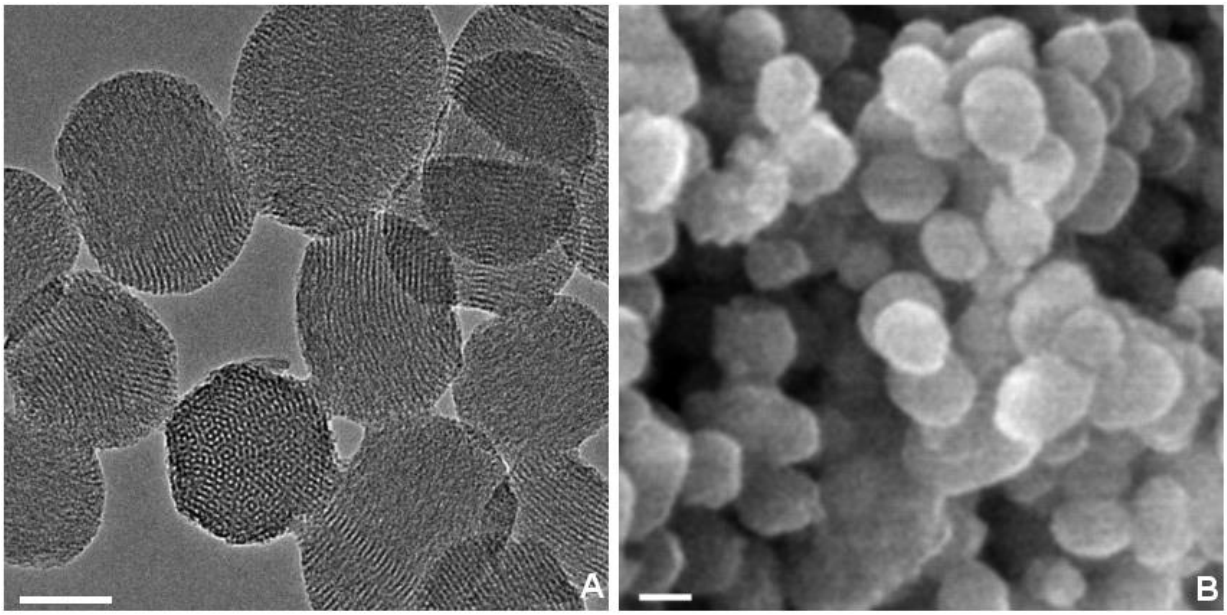

Figure 1 - Characterisation of mesoporous silica nanoparticles (MSNPs). (A) Transmission electron microscopy image of unmodified MSNPs. Scalebar = 0.05 μm; (B) Scanning electron microscopy image of unmodified MSNPs. Scalebar = 0.1 μm. Synthesised MSNPs were characterised by homogenous size, slightly non-spherical shape with elongation in the direction of the pore channels, and nanometre-sized pores with hexagonal symmetry (reproduced from [21] with permission).

Functionalisation of MSNPs with C105Y had little effect upon ζ potential in incubation medium (-11.23±1.05 mV versus -11.57±0.56 mV for unmodified and C105Y-functionalised MSNPs, respectively), and slightly increased their hydrodynamic size in PBS (290±47.2nm versus 322±21.5nm for unmodified and

C105Y-functionalised MSNPs, respectively). Calculated peptide:MSNP binding ratio was approximately 0.5nmol of C105Y per 10μg of MSNPs.

3.2. Sperm motility and morphology after exposure to C105Y-functionalised MSNPs and free C105Y

Sperm motility, kinematic parameters and the proportion of sperm with NAR were evaluated using CASA and high-magnification microscopy after 2 hours of incubation with C105Y-functionalised MSNPs at ratios of 10, 15 and 30μg of particles per 10^7 sperm, or equivalent doses of free C105Y, and compared to time-matched controls. Exposure to C105Y-functionalised MSNPs in all nanoparticle/sperm ratios, and equivalent doses of free C105Y, did not result in a significant negative effect upon the total and progressive motility of boar sperm on a population level across all samples (Figures 2A and 2B). Neither treatment resulted in a significant change in the kinematic parameters of sperm, compared to time-matched controls (Figures 2D-2E). Similarly, a proportion of sperm with NAR, evaluated by high-magnification light microscopy, approximated the reference threshold of 80% across all experimental groups exposed to C105Y-functionalised MSNPs, or free C105Y, and did not deviate significantly from the control group (Figure 2C).

Interestingly, a separate logistic regression analysis of individual boar sperm data (N=19880) demonstrated a protective effect of both C105Y-functionalised MSNPs, and free C105Y, upon total sperm motility (Table 1). The probability for an individual sperm to exhibit motility after 2 hours of incubation with MSNPs+C105Y, or free C105Y, versus time-matched controls increased by almost 18% (OR: 1.177;

$p<0.05$) and 20% (OR: 1.203; $p<0.05$), respectively. Similarly, a one-unit increase of the dose of MSNPs+C105Y/free C105Y resulted in an approximately 1% (OR: 1.008) increment in the probability of observing motility in an individual sperm. In contrast, for progressive motility, exposure to C105Y-functionalised MSNPs, but not free C105Y, significantly reduced the likelihood for an individual sperm to move in a progressive fashion after 2 hours of incubation (-15.2%; OR: 0.848; $p<0.05$), compared to controls. This observation prompted further assessment of the effect of both experimental agents upon the sub-proportions of 'rapid' sperm, which move within the same velocity range, but in a less straight fashion (VSL/VAP<45%). In this analysis, no significant effect of either C105Y-functionalised MSNPs, or free C105Y, was demonstrated with regard to the probability of an individual sperm exhibiting 'rapid' motility. Collectively, these findings could indicate that on an individual sperm level, binding of C105Y-functionalised MSNPs prevents sperm from moving at the highest velocity with straight-line trajectory ('progressive'), but does not affect the probability of sperm to exhibit motility in general, including the 'rapid' classification

Exposure to C105Y-functionalised MSNPs also served as a protective factor for boar acrosome morphology. In logistic regression analysis of data from 2220 individual sperm, the probability of sperm to demonstrate a normal apical ridge following incubation with C105Y-functionalised MSNPs increased by 75% (OR: 1.750, $p<0.05$) versus controls. No similar effect was observed in the free C105Y group.

Table 1 – Odds ratios for observing motility, progressive motility and NAR in individual sperm after 2 hours of exposure to C105Y-functionalised MSNPs or free C105Y*

Outcome		Odds Ratio	95% Confidence Interval for Odds Ratio		P
			Lower	Upper	
Motility[a] (N=12450)	Type:				.004
	MSNPs+C105Y	1.177	1.060	1.307	.002
	Free C105Y	1.203	1.073	1.349	.002
	Dose	1.008	1.004	1.013	.000
Progressive motility[b] (N=4197)	Type:				.024
	MSNPs+C105Y	0.848	0.751	0.958	.008
	Free C105Y	0.896	0.788	1.018	*NS*
	Dose	1.001	0.996	1.006	*NS*
Rapid sperm[c] (N=4569)	Type:				*NS*
	MSNPs+C105Y	0.945	0.839	1.063	*NS*
	Free C105Y	0.980	0.866	1.110	*NS*
	Dose	1.001	0.996	1.005	*NS*
Normal apical ridge[d] (N=1739).	Type:				.000
	MSNPs+C105Y	1.750	1.137	2.694	.011
	Free C105Y	0.905	0.596	1.377	*NS*
	Dose	1.001	0.987	1.016	*NS*

* Control group used as a reference category; NS: not significant. Analysis included individual motility data for 19880 sperm, and individual acrosome morphology data for 2220 sperm. [a] $\chi^2_7 = 1027.955$, $p<0.05$, correct classification: 63.5% of cases; [b] $\chi^2_7 = 747.513$, $p<0.05$, correct classification: 75.8% of cases; [c] $\chi^2_7 = 600.749$, $p<0.05$, correct classification: 73.7% of cases; [d] $\chi^2_5 = 35.720$, $p<0.05$; correct classification: 82.2% of cases.

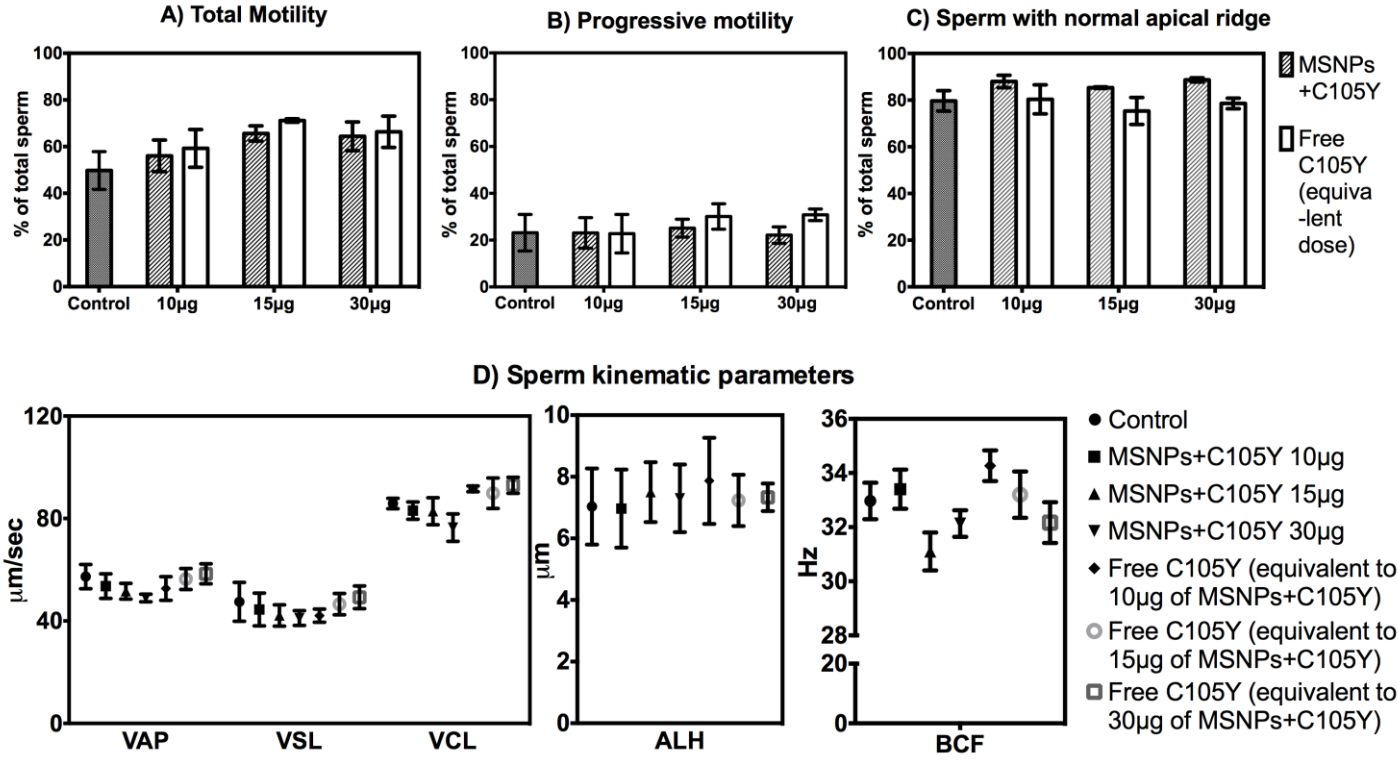

Figure 2 – Motility, kinematic parameters and acrosome morphology of boar sperm assessed by CASA and high-magnification microscopy after 2 hours of exposure to C105Y-functionalised MSNPs in various particle/cell ratios or equivalent doses of free C105Y. VAP: smoothed path velocity; VSL: straight line velocity; VCL: track velocity; ALH: amplitude of lateral head displacement; BCF: beat cross frequency. For motility and kinematic parameters, data are presented as mean ± SEM from five samples for controls and MSNPs+C105Y, and three samples for free C105Y. For acrosome morphology, data presented as mean ± SEM from three samples control and experimental samples. On the sample level, sperm motility, morphology and kinematic parameters after exposure to C105Y-functionalised MSNPs/free C105Y remained unaltered, compared to time-matched controls ($p>0.05$).

3.3. Association of C105Y-functionalised MSNPs with sperm

Association rates between boar sperm and C105Y-functionalised MSNPs were assessed after 1 and 2 hours of exposure, in accordance with our previous findings, indicating that stable adsorption of MSNPs to the sperm surface occurred after just 2 hours of incubation *in vitro*. Similarly to our earlier observations, C105Y-functionalised MSNPs bound to various sperm regions, including the head, mid-piece and tail, and emitted sharp and focused fluorescent signals on a dark or homogenously stained fluorescent background of variable intensity (Figure 3). In some sperm, binding of C105Y-functionalised MSNPs followed a distinctive localisation profile of free C105Y, which demonstrated high affinity towards the post-equatorial region of the sperm head and posterior ring (junction of head and mid-piece).

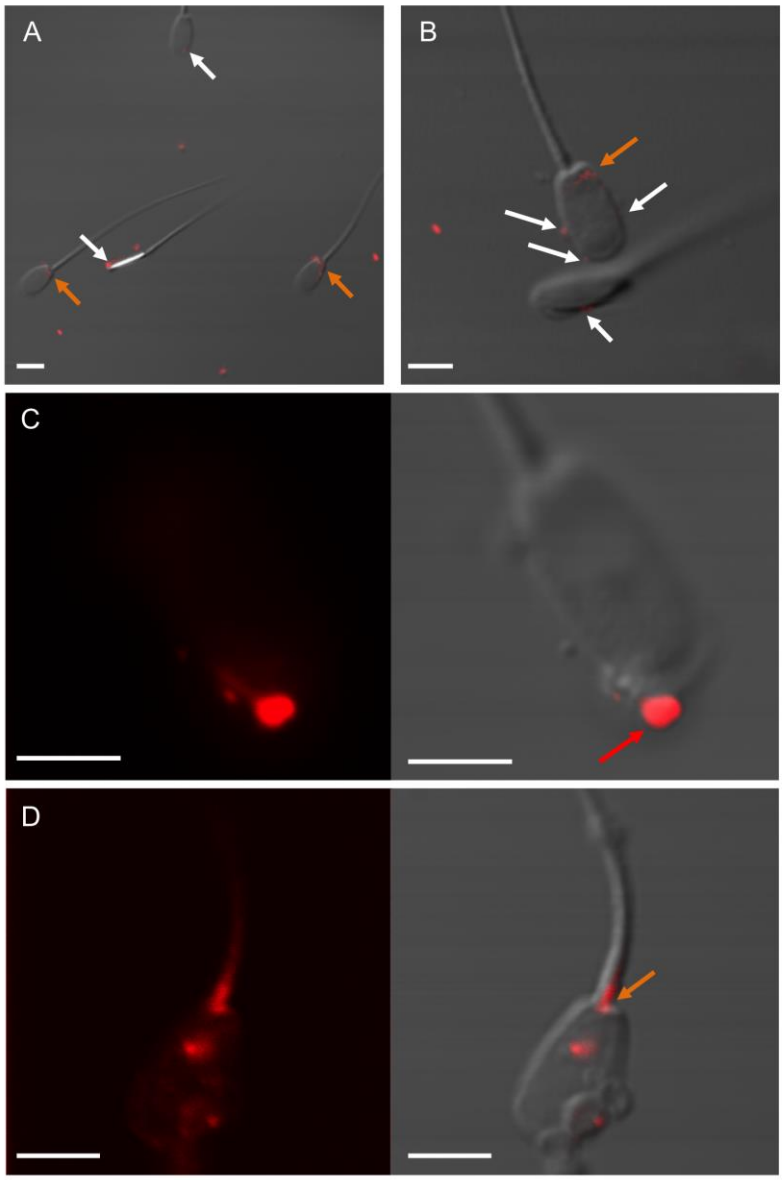

Figure 3 – Association of C105Y-functionalised MSNPs with boar sperm. Scalebar = 5 µm. A-B) C105Y-functionalised MSNPs associated with sperm emit sharp and focused fluorescent signals in the projection of various sperm regions (white arrows indicate MSNP-sperm associations; orange arrows indicate associations in post-equatorial region of the head and posterior ring). C-D) Association of C105Y-functionalised MSNPs with sperm. MSNPs bind to the sperm head and midpiece, and produce a sharp fluorescent signal on a dark or homogenously stained fluorescent background (red arrow indicates a large agglomerate of MSNPs)

Association rate between sperm and C105Y-functionalised MSNPs was significantly dependent upon the dose of nanoparticles ($F_{1,19}$=20.600, $p<0.05$), but not the time of exposure (Figure 4). An increase in particle/sperm ratio from 10µg to 30µg per 10^7 sperm improved the association rate at both incubation time points by almost a

third (23.7±2.7% vs 38.3±0.6% at 1 hour, and 25.4±1.8% vs 35.9±2.2% at 2 hours). At the same time, an increase in the duration of incubation from 1 to 2 hours did not markedly enhance particle-sperm binding. Analysis of individual sperm data (N=4749, χ^2_6 = 97.924, $p<0.05$, correct classification: 68.3% of cases) further confirmed these findings, indicating that the probability of observing binding with C105Y-functionalised MSNPs in an individual sperm increased by almost 3% per each one-unit increment of the applied dose of C105Y-functionalised MSNPs (OR: 1.028; 95%CI [1.020-1.035]; $p<0.05$).

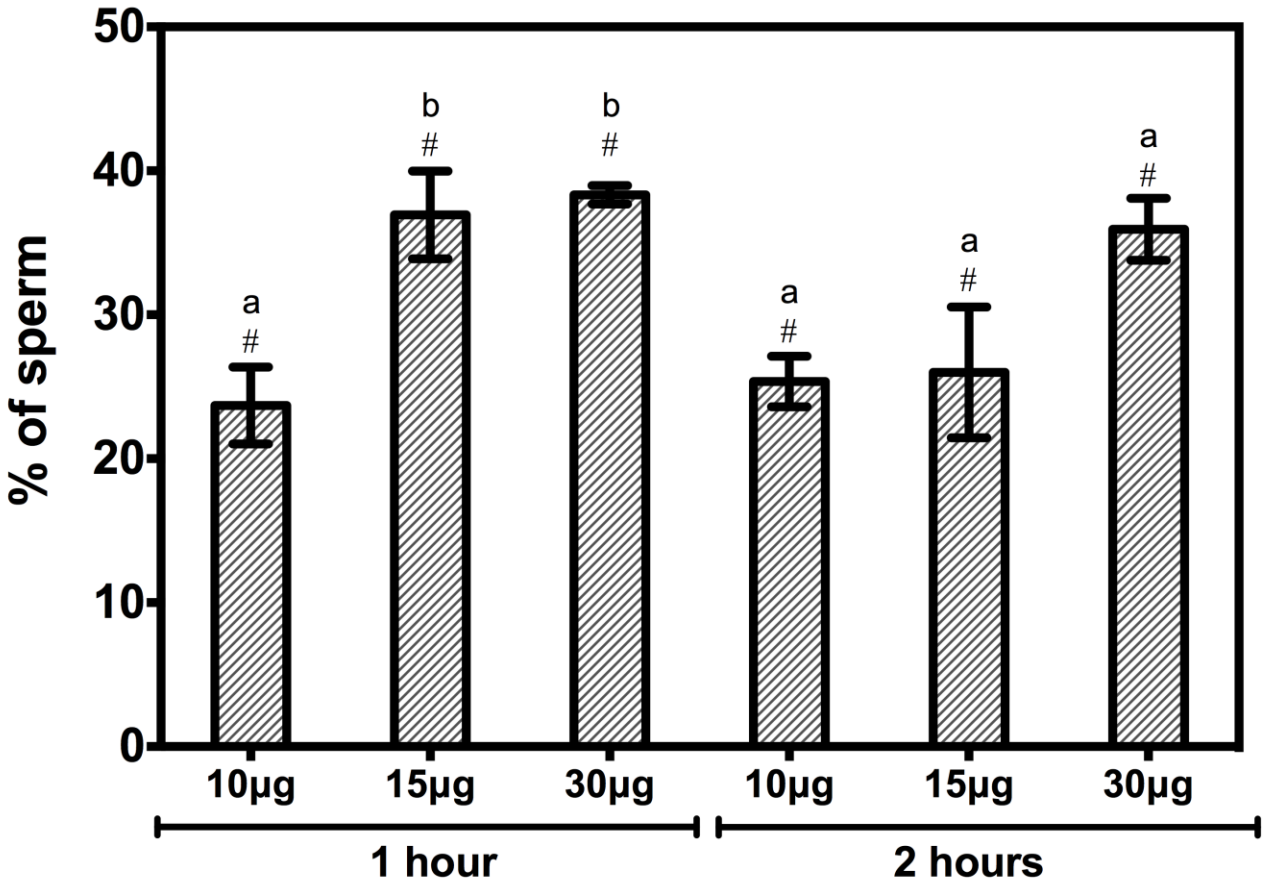

Figure 4 – Association rates between C105Y-functionalised MSNPs and boar sperm after 1 and 2 hours of incubation *in vitro* in various particle/cell ratios. Data presented as mean±SEM from five samples. Each letter (a,b) denotes a subset of three dose categories within the same time point, whose values do not differ significantly from each other at the 0.05 level. Symbol (#) denotes a subset of same dose categories at two different time points, whose values do not differ significantly from each other at the 0.05 level.

To evaluate the effects of functionalisation upon the binding capacity between MSNPs and boar sperm, the association rates of C105Y-functionalised MSNPs were compared with retrospective data for unmodified MSNPs, obtained under similar conditions, and controlled for inter-sample variability (Table 2). A significant effect of type ($F_{1,37}$=12.100; p<0.05) and dose of nanoparticles ($F_{1,37}$=22.170, p<0.05) upon association rate was observed. Binding of MSNPs with sperm was significantly promoted by the functionalisation of MSNPs with C105Y (fixed coefficient for MSNPs vs MSNPs+C105Y: -11.110; 95%CI [-17.582;-4.639]; p<0.05) and an increase in the dose of unmodified MSNPs (fixed coefficient: 0.692; 95%CI [0.394; 0.989], p<0.05). Functionalisation of MSNPs with C105Y markedly increased association rates with boar sperm, especially during the early stages of incubation, where an approximately 3- to 4-fold mean increment was observed, allowing binding levels to be achieved that were similar to those after 2 hours of exposure to unmodified MSNPs, after just 1 hour of treatment.

Table 2 - Association rates between sperm and C105Y-functionalised/unmodified MSNPs

	1 hour			**2 hours**		
	Unmodified MSNPs	C105Y-functionalised MSNPs	P	Unmodified MSNPs	C105Y-functionalised MSNPs	P
MSNP/sperm ratio:						
10ug per 10^7 sperm	7.4±1.7%	23.7±2.7%	<0.05	17.4±1.9%	25.4±1.8%	*NS*
15ug per 10^7 sperm	6.4±4.4%	36.9±3.0%	<0.05	20.8±5.7%	26.0±4.5%	*NS*
30ug per 10^7 sperm	14.5±1.0%	38.3±0.6%	<0.05	41.0±9.2%	35.9±2.2%	*NS*

NS=not significant

3.4. Cell fluorescence after exposure to C105Y-functionalised MSNPs and free C105Y

Cell fluorescence levels in sperm exposed to C105Y-functionalised MSNPs and equivalent doses of free C105Y were quantified after 1 and 2 hours of incubation to evaluate the effects of absorption of C105Y on a nanocarrier upon its transport into sperm. Accumulation of free C105Y in boar sperm was consistent with a previously described pattern for bull sperm: C105Y localised primarily to the post-equatorial region of the sperm head, posterior ring and mid-piece [29]. Analysis of cell fluorescence levels, corrected for background fluorescence and expressed as arbitrary units (AU) per 1 μm^2 of sperm surface area, demonstrated a significant effect of the type of treatment ($F_{1,1151}$=51.338; $p<0.05$), dose of nanoparticles/free peptide ($F_{1,1151}$= 75.054, $p<0.05$) and time of exposure ($F_{1,1151}$=91.961, $p<0.05$) upon fluorescence intensity.

Exposure of sperm to C105Y-functionalised MSNPs resulted in significantly increased levels of cell fluorescence, compared to free C105Y, across all dose ratios and incubation time points (Figure 5). In most cases, levels of cell fluorescence following exposure to the smallest dose ratio of C105Y-functionalised MSNPs (10μg per 10^7 sperm), or free C105Y, were significantly different than the two larger dose ratios (15μg and 30μg per 10^7 sperm). Corrected fluorescence intensity in sperm exposed to C105Y-functionalised MSNPs remained relatively stable throughout the incubation period. However, in the free C105Y group, a reduction of cell fluorescence at the 2-hour versus 1-hour incubation time point in the 15μg- and 30μg-equivalent groups was observed.

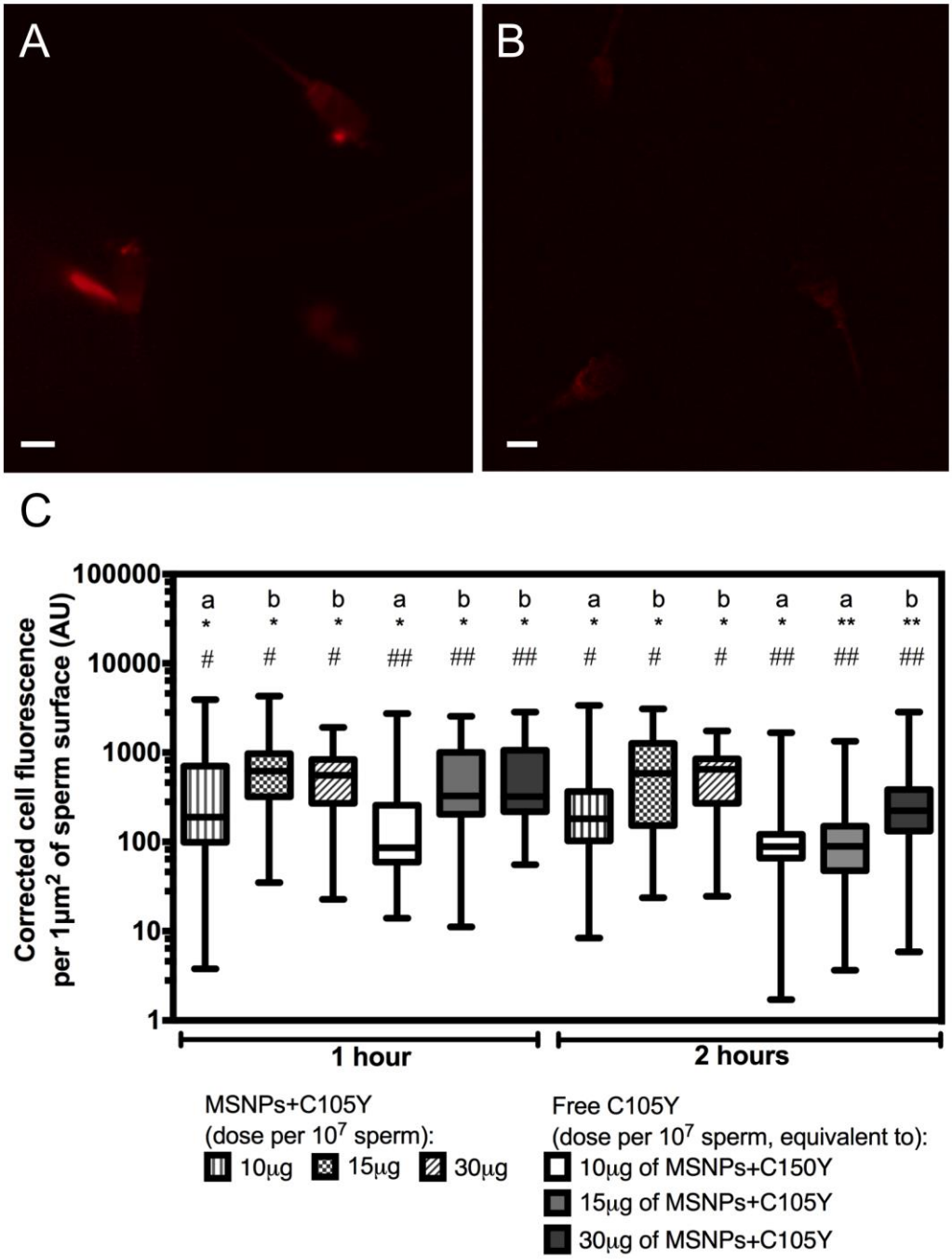

Figure 5 – Cell fluorescence after exposure to C105Y-functionalised MSNPs or equivalent doses of free C105Y. A) Sperm after exposure C105Y-functionalised MSNPs in a 10µg per 10^7 cells ratio. B) Sperm after exposure to free C105Y in a dose, equivalent to absorbed on 10µg of C105Y-funtionalised MSNPs.Scalebar = 5µm. C) Levels of corrected cell fluorescence per $1\mu m^2$ of sperm surface area. Box plots represent distributions (median; min-max) of corrected cell florescence per $1\mu m^2$ of surface area of individual sperm from six samples. Each letter (a,b) denotes a subset of three dose categories of each experimental agent within the same time point (i.e. 10 µg vs 15µg vs 30µg of MSNPs+C105Y at 1 hour), whose values do not differ significantly from each other at the 0.05 level. Symbol (*) denotes a subset of same dose categories of each experimental agent at two different time points (i.e. 10 µg of MSNPs+C105Y at 1 hour vs 2 hours) whose values do not differ significantly from each other at the 0.05 level. Symbol (#) denotes a subset of same dose categories of two different experimental agents at the same time point (i.e. 10 µg of MSNPs+C105Y vs an equivalent dose of free C105Y at 1 hour), whose values do not differ significantly from each other at the 0.05 level.

4. DISCUSSION

In recent years, various nanotechnology tools have been increasingly investigated for targeted delivery in reproductive biology, in order to facilitate the specific and controllable transport of large amounts of various payloads into reproductive tissues, gametes and embryos for experimental research, diagnostics and therapy [2]. From the reproductive biology perspective, the main strength of nanomaterials lies in their universally recognised ability to improve the internalisation of exogenous cargo into cells. Reproductive tissues and gametes, particularly sperm, are characterised by highly specialised morphology and function with substantial levels of physiological resistance towards the uptake of molecular cargo [9], which can limit performance of research methodologies requiring the transport of investigative compounds inside these cells. Currently, the main approach for improving intracellular uptake in sperm is artificial permeabilisation of cell membranes with detergents – an aggressive technique which can detrimentally affect the DNA structural integrity and developmental capacity of gametes [34, 35] and is poorly compatible with experiments investigating the fine mechanisms of fertilisation and subsequent embryo development.

It is therefore not surprising that the idea of nanomaterial-mediated delivery into gametes and embryos as a seemingly safer and 'milder' alternative to conventional techniques has been increasingly explored over the last decade. In a series of animal *in vitro* and *in vivo* studies, polyvinylalcohol-functionalised iron oxide [16, 36], magnetic [13] and polystyrene/polyacrilonitryl nanoparticles [37], halloysite clay nanotubes and commercial polymeric nanotransfectants [14, 15], and specialised CdSe/ZnS quantum

dots [17] have been characterised as safe and effective tools for a number of research techniques in reproductive biology, including the transfer of nucleic acid/protein into sperm, labelling of embryos in culture during *in vitro* fertilisation, experimental *in utero* gene therapy, and sperm bioimaging. It is, however, of particular worth to note, that the biocompatibility of well-established nanomaterials with gametes, for example nanogold, often differs substantially from that with somatic cells, and has been reported to produce unexpected negative outcomes [19, 38, 39].

In a recent study, we demonstrated that mesoporous silica is biocompatible with mammalian sperm and forms strong associations with approximately one in four cells after simple incubation *in vitro*, adding spherical MSNPs with hexagonal pore symmetry to a subset of potential compound transfer vehicles for reproductive biology [21]. Indeed, mesoporous silica possesses a number of features, rendering it a promising candidate nanocarrier for reproductive research. These features include robustness, chemical inertness, versatility, ease of manufacturing, and, finally, unique porous architecture, which dramatically increases the available surface area and creates an additional, intra-porous, compartment for cargo loading [20]. Although previous studies have not specifically quantified the proportion of sperm demonstrating binding with nanoparticles, but rather focused on the proportion of nanoparticles bound, the association rates observed in our first study appeared relatively low. However, from the perspective of reproductive biology, particularly for experiments involving the sperm-mediated delivery of compounds into the oocyte at the time of fertilisation, the likelihood of transport is directly proportionate to the number of nanoparticle-carrying

sperm, and, therefore, the actual size of the sperm cohort carrying particles appears to play an important role. This vision justified further research into the potential strategies to improve MSNP-sperm association.

Our current study aimed to investigate the effects of the functionalization of MSNPs with a 17-amino acid synthetic poly-cationic cell-penetrating peptide C105Y (CSIPPEVKFNKPFVYLI) [28], upon the binding of MSNPs with boar sperm. The specific choice of C105Y for surface functionalization of MSNPs has been driven, firstly, by the encouraging evidence of its high affinity towards mammalian sperm, compared to a subset of another 13 well-characterised CPPs, including penetratin, Tat and mitoparan [29], and, secondly, its proposed energy- and receptor-independent internalisation profile. The sperm membrane is highly compartmentalised and undergoes continuous dynamic changes during the events preceding fertilisation [40]; therefore, the availability of a functionalization agent, which would not interact with a particular subset of surface receptors and potentially interfere with these dynamic modifications, is highly favourable. In this study, we continued to use the term ‘association’ to collectively describe both surface binding and potential internalisation as a positive outcome of interaction between MSNPs and sperm. There is growing evidence that the uptake of nanomaterials by gametes is not as straightforward as that of somatic cells: most publications describe surface attachment or sequestration within the plasma membrane as the primary outcome of exposure of gametes to nanomaterials, with only a very small proportion of nanocarrier reaching the intracellular compartment [13, 17-19, 36, 37], and in some cases, none at all Nevertheless, such profiles of

interaction do not seem to compromise the performance of research techniquesbased upon such methodologies, and therefore, the precise mapping of C105Y-functionalised MSNPs was beyond the scope of this set of experiments.

Our results show that functionalization of MSNPs with the sperm-specific cell-penetrating peptide C105Y increases MSNP-sperm association rate, and represents a viable strategy in the arsenal of reproductive biology. In this study, C105Y-functionalised MSNPs started to form stable associations with boar sperm after as little as 1 hour of exposure, compared to 2 hours for unmodified MSNPs. Interestingly, the proportion of sperm demonstrating binding with C105Y-functionalised nanoparticles was significantly increased compared to unmodified MSNPs after only 1 hour of exposure, indicating an increased affinity of functionalised MSNPs towards sperm during the early stages of incubation. After 2 hours, although association rates for C105Y-functionalised MSNPs were mostly higher compared to unmodified particles, the difference no longer reached statistical significance. At this point, association rates in both groups stabilised at a plateau of approximately 20%-30%, which was consistent with the results of our previous study. This observation could indicate that binding with MSNPs occurs primarily in a certain subset of sperm, and that functionalization of nanoparticles with C105Y aids with initial ‘anchoring’ of MSNPs onto the surface of these cells, but not in the entire sperm population. Unfortunately, interpretation of our results in the context of available evidence remains challenging. Although the functionalization of nanoparticles with CPP has been attempted previously [17], this earlier study utilised a different nanomaterial and CPP (CdSe/ZnS quantum dots

functionalized with nona-Arginine R9 peptide), and did not quantify the overall size of sperm population associated with nanoparticles or variations in binding rate compared to unmodified nanomaterial.

In the present study, functionalisation of MSNPs with C105Y resulted in a change of association pattern with boar sperm, with selected cells demonstrating binding of MSNPs in the post-equatorial region of the sperm head and posterior ring – a profile previously described for free C105Y and rarely documented for unmodified MSNPs. This observation supports the hypothesis that functionalization of MSNPs with a cell-specific moiety is likely to alter their binding profile with a specific target.

We observed that exposure of sperm to C105Y adsorbed on MSNPs consistently resulted in a significant increase of corrected cell fluorescence levels per 1 μm^2 of sperm surface area compared to free C105Y, across all dose ratios and incubation time points. Nanoparticles have been previously reported to promote the uptake of exogenous DNA into sperm in nanoSMGT experiments [13-15], compared to standard SMGT, however similar comparative studies with intracellular transport of proteins and peptides have yet to be carried out. Even though the internalisation of nanomaterials into sperm in nanoSMGT experiments did not occur consistently, the efficacy of cargo delivery was increased, perhaps due to structural modifications of the plasma membrane following contact with nanoparticles [19]. Interestingly, we observed a reduction in cell fluorescence at the 2-hour versus 1-hour incubation time point in the free C105Y group (15μg- and 30μg per 10^7 sperm equivalent groups), a new finding which cannot be

readily interpreted since previous experiments evaluated the delivery of C105Y into sperm only after 1 hour incubation [29].

Finally, in our study, functionalization of MSNPs with C105Y did not affect the biocompatibility of mesoporous silica with boar sperm. Although both compounds have been tested for gametotoxicity previously [21, 29], confirmation of the biological safety of functionalised MSNPs in sperm remains an essential step, since previous reports have highlighted the detrimental effects of surface modification of nanomaterials, such as the removal of coatings or functionalization moieties, upon their toxicity profiles in gametes [19, 41]. In this set of experiments, no negative effects upon total and progressive motility, kinematic parameters of sperm, and proportion of cell with NAR were observed at the sample level following exposure to various doses of C105Y-functionalised MSNPs, and equivalent amounts of free C105Y, compared to the control group. Additionally, we carried out separate logistic regression analysis of individual sperm data, accounting for inter-sample variability, to investigate the effects of exposure upon cells in greater detail. Interestingly, this analysis indicated a protective effect of both compounds upon total sperm motility, and a beneficial role of C105Y-functionalised MSNPs upon the integrity of the acrosomal apical ridge. This observation could be partially explained by the reported ability of mesoporous silica to supress production of endogenous reactive oxygen species [42], a powerful source of sperm oxidative damage. However, given the scarce nature of such reports, this phenomenon requires further investigation. Another interesting outcome of the analysis of individual sperm data was the isolated negative effect of C105Y-functionalised

MSNPs, but not free C105Y, upon progressive motility (VAP>45μm/sec; VSL/VAP>45%), without a similar effect upon the probability to assign sperm to a 'rapid' motility category (VAP>45μm/sec; VSL/VAP<45%). These results suggest that on an individual sperm level, the physical binding of MSNPs does not necessarily result in sperm retardation, but rather changes its swimming trajectory. In our study, the protective effects of C105Y-functionalised MSNPs, and free C105Y, upon total sperm motility, the beneficial effects of C105Y-functionalised MSNPs upon the integrity of acrosomal apical ridge, and the isolated negative effect upon progressive, were detected at the individual sperm level, but not at the sample level. This discrepancy could be explained by the pilot nature of this study and a relatively small sample size, thus justifying further investigation in a larger dataset.

CONCLUSIONS

In this study, for the first time, we report the use of a 17-amino acid synthetic poly-cationic peptide, C105Y, with affinity towards mammalian sperm, for the functionalization of spherical MSNPs with hexagonal pore symmetry, and the subsequent use of these functionalised MSNPs in boar sperm. Functionalization of MSNPS with C105Y enhanced their ability to form strong associations with sperm following incubation *in vitro*, allowing for earlier binding with the sperm surface, compared to unmodified MSNPs, and the establishment of new binding profiles. The exposure of sperm to MSNP-absorbed C105Y resulted in a significant increase in cell fluorescence levels, compared to free peptide, highlighting a potential effect of

nanoparticles upon the permeability of the sperm membrane. Finally, C105Y-functionalised MSNPs retain biocompatibility with mammalian sperm from the perspective of total motility and acrosome morphology, although interference with the trajectory of sperm motion at the individual sperm level, due to anchoring of MSNPs to the surface membrane, cannot be excluded. Collectively, these findings support the position of mesoporous silica as a potential delivery vector for reproductive biology and indicate that specific targeting towards sperm represents a viable tool to promote favourable outcomes of interaction between gametes and nanomaterials.

SUMMARY POINTS

- Functionalisation of spherical mesoporous silica nanoparticles with hexagonal pore symmetry with a 17-amino acid synthetic poly-cationic cell-penetrating peptide C105Y increases their affinity towards sperm.

- C105Y-functionalised MSNPs form strong associations with sperm at much earlier time points, compared to unmodified MSNPs, and, in certain cases, demonstrate binding profiles similar to that of free C105Y.

- The peak association rate between C105Y-functionalised MSNPs and sperm remained relatively unchanged compared to unmodified MSNPs, indicating that binding with particles can be restricted to a particular sperm sub-population.

- Adsorption of C105Y on MSNPs resulted in increased levels of cell fluorescence compared to free C105Y which could suggest that MSNPs increase permeability of sperm membrane.

- C105Y-functionalised MSNPs remain biocompatible with sperm and, on a sample level, do not impart a negative effect upon sperm motility and morphology; however, binding can interfere with the trajectory of sperm movement on an individual sperm level.

- Specific targeting towards gametes represents a viable tool to promote favourable outcomes of interaction between these specialised cells and nanomaterials.

FIGURES AND FIGURE LEGENDS

Figure 1 - Characterisation of mesoporous silica nanoparticles (MSNPs). (A) Transmission electron microscopy image of unmodified MSNPs. Scalebar = 0.05 μm; (B) Scanning electron microscopy image of unmodified MSNPs. Scalebar = 0.1 μm. Synthesised MSNPs were characterised by homogenous size, slightly non-spherical shape with elongation in the direction of the pore channels, and nanometre-sized pores with hexagonal symmetry (reproduced from [21] with permission).

Figure 2 – Motility, kinematic parameters and acrosome morphology of boar sperm assessed by CASA and high-magnification microscopy after 2 hours of exposure to C105Y-functionalised MSNPs in various particle/cell ratios or equivalent doses of free C105Y. VAP: smoothed path velocity; VSL: straight line velocity; VCL: track velocity; ALH: amplitude of lateral head displacement; BCF: beat cross frequency. For motility and kinematic parameters, data are presented as mean ± SEM from five samples for controls and MSNPs+C105Y, and three samples for free C105Y. For acrosome morphology, data presented as mean ± SEM from three samples control and experimental samples. On the sample level, sperm motility, morphology and kinematic parameters after exposure to C105Y-functionalised MSNPs/free C105Y remained unaltered, compared to time-matched controls ($p>0.05$).

Figure 3 – Association of C105Y-functionalised MSNPs with boar sperm. Scalebar = 5 μm. A-B) C105Y-functionalised MSNPs associated with sperm emit

sharp and focused fluorescent signals in the projection of various sperm regions (white arrows indicate MSNP-sperm associations; orange arrows indicate associations in post-equatorial region of the head and posterior ring). C-D) Association of C105Y-functionalised MSNPs with sperm. MSNPs bind to the sperm head and midpiece, and produce a sharp fluorescent signal on a dark or homogenously stained fluorescent background.

Figure 4 – Association rates between C105Y-functionalised MSNPs and boar sperm after 1 and 2 hours of incubation *in vitro* in various particle/cell ratios. Data presented as mean±SEM from five samples. Each letter (a,b) denotes a subset of three dose categories within the same time point, whose values do not differ significantly from each other at the 0.05 level. Symbol (#) denotes a subset of same dose categories at two different time points, whose values do not differ significantly from each other at the 0.05 level.

Figure 5 – Cell fluorescence after exposure to C105Y-functionalised MSNPs or equivalent doses of free C105Y. A) Sperm after exposure C105Y-functionalised MSNPs in a 10μg per 10^7 cells ratio. B) Sperm after exposure to free C105Y in a dose, equivalent to absorbed on 10μg of C105Y-funtionalised MSNPs.Scalebar = 5μm. C) Levels of corrected cell fluorescence per 1μm^2 of sperm surface area. Box plots represent distributions (median; min-max) of corrected cell florescence per 1μm^2 of surface area of individual sperm from six samples. Each letter (a,b) denotes a subset of

three dose categories of each experimental agent within the same time point (i.e. 10 μg vs 15μg vs 30μg of MSNPs+C105Y at 1 hour), whose values do not differ significantly from each other at the 0.05 level. Symbol (*) denotes a subset of same dose categories of each experimental agent at two different time points (i.e. 10 μg of MSNPs+C105Y at 1 hour vs 2 hours) whose values do not differ significantly from each other at the 0.05 level. Symbol (#) denotes a subset of same dose categories of two different experimental agents at the same time point (i.e. 10 μg of MSNPs+C105Y vs an equivalent dose of free C105Y at 1 hour), whose values do not differ significantly from each other at the 0.05 level.

REFERENCE ANNOTATIONS

[13] Original research paper describing the use of magnetic nanoparticles to aid sperm-mediated reporter gene transfer into porcine embryos.

[14] Original research paper describing the use of halloysite clay nanotubes and commercial biopolymer for the nanotransfection of bull sperm and subsequent transfer of exogenous DNA into bovine embryos.

[16] The first original research paper presenting the results of a study involving successul intra-sperm transfer of a protein using iron oxide nanoparticles in a bovine model.

[17] The first original research paper utilizing specialised quantum dots functionalised with a cell-penetrating peptide for live bioimaging of boar sperm.

[19] Original research paper, evaluating the spacial localisation of gold nanoparticles in sperm after exposure *in vitro*, and the effects of exposure upon the structure and function of the sperm membrane and developmental potential of resulting embryos.

[21] Original research paper, demonstraing biocompatibility of mesoporous silica nanoparticles with mammalian sperm, which formed the basis for the current study.

[29] Original research paper, evaluating the uptake of a series of cell-penetrating peptides into mammalian sperm, and identifying C105Y as a promising candidate for sperm biology studies.

FINANCIAL DISCLOSURES/ACKNOWLEDGEMENTS

The authors wish to acknowledge Miss Rachel Morrisson, Ms Cindy Huang, and Dr Marc Yeste for their support, and Dr Christopher Gardiner for his help in characterising the nanoparticles. The authors have a patent pending related to the work discussed in this article entitled ‘Delivery Method’ (PCT Patent Application Number PCT/GB13/053394 filed on the 20th December 2013). Natalia Barkalina is funded by the Clarendon, Scatcherd European and Cyril & Phillis Long Schemes. The project is also funded by the Nuffield Department of Obstetrics and Gynaecology, and an EPSRC Pathways to Impact Award (University of Oxford). The authors have no other relevant affiliations or financial involvement with any organization or entity with a financial interest in, or financial conflict with, the subject matter or materials discussed in the manuscript. This includes employment, consultancies, honoraria, stock ownership or

options, expert testimony, grants or patents received or pending, or royalties. No writing assistance was utilized in the production of this manuscript.

REFERENCES

1. Tsai N, Lee B, Kim A *et al.*: Nanomedicine for Global Health. *Journal of Laboratory Automation* 10.1177/2211068214538263, (2014).
2. Barkalina N, Charalambous C, Jones C, Coward K: Nanotechnology in reproductive medicine: Emerging applications of nanomaterials. *Nanomedicine: Nanotechnology, Biology and Medicine* 10(5), 921-938 (2014).
3. Ikawa M, Tergaonkar V, Ogura A, Ogonuki N, Inoue K, Verma IM: Restoration of spermatogenesis by lentiviral gene transfer: Offspring from infertile mice. *Proceedings of the National Academy of Sciences of the United States of America* 99(11), 7524-7529 (2002).
4. Ghadami M, El-Demerdash E, Salama SA *et al.*: Toward gene therapy of premature ovarian failure: intraovarian injection of adenovirus expressing human FSH receptor restores folliculogenesis in FSHR(-/-) FORKO mice. *Mol Hum Reprod* 16(4), 241-250 (2010).
5. Brackett BG: Uptake of heterologous genome by mammalian spermatozoa and its transfer to ova through fertilization. *Proceedings of the National Academy of Sciences of the United States of America* 68(2), 353-357 (1971).
6. Rath D, Barcikowski S, de Graaf S *et al.*: Sex selection of sperm in farm animals: status report and developmental prospects. *Reproduction* 145(1), R15-R30 (2013).
7. Kojima Y, Hayashi Y, Kurokawa S, Mizuno K, Sasaki S, Kohri K: No evidence of germ-line transmission by adenovirus-mediated gene transfer to mouse testes. *Fertil Steril* 89(Suppl 5), 1448-1454 (2008).
8. Eghbalsaied S, Ghaedi K, Laible G *et al.*: Exposure to DNA is insufficient for in vitro transgenesis of live bovine sperm and embryos. *Reproduction* 145(1), 97-108 (2013).
9. Gadella BM, Evans JP: Membrane fusions during mammalian fertilization. *Adv Exp Med Biol* 713, 65-80 (2011).
10. Sullivan R, Saez F: Epididymosomes, prostasomes, and liposomes: their roles in mammalian male reproductive physiology. *Reproduction* 146(1), R21-35 (2013).
11. Caballero JN, Frenette G, Belleannee C, Sullivan R: CD9-positive microvesicles mediate the transfer of molecules to Bovine Spermatozoa during epididymal maturation. *PLoS One* 8(6), e65364 (2013).
12. Sohel MM, Hoelker M, Noferesti SS *et al.*: Exosomal and Non-Exosomal Transport of Extra-Cellular microRNAs in Follicular Fluid: Implications for Bovine Oocyte Developmental Competence. *PLoS One* 8(11), e78505 (2013).
13. Kim TS, Lee SH, Gang GT *et al.*: Exogenous DNA uptake of boar spermatozoa by a magnetic nanoparticle vector system. *Reprod Domest Anim* 45(5), e201-206 (2010).
14. Campos VF, de Leon PMM, Komninou ER *et al.*: NanoSMGT: Transgene transmission into bovine embryos using halloysite clay nanotubes or nanopolymer to improve transfection efficiency. *Theriogenology* 76(8), 1552-1560 (2011).
15. Campos VF, Komninou ER, Urtiaga G *et al.*: NanoSMGT: transfection of exogenous DNA on sex-sorted bovine sperm using nanopolymer. *Theriogenology* 75(8), 1476-1481 (2011).
16. Makhluf SB, Abu-Mukh R, Rubinstein S, Breitbart H, Gedanken A: Modified PVA-Fe3O4 nanoparticles as protein carriers into sperm cells. *Small* 4(9), 1453-1458 (2008).
17. Feugang JM, Youngblood RC, Greene JM *et al.*: Application of quantum dot nanoparticles for potential non-invasive bio-imaging of mammalian spermatozoa. *J Nanobiotechnology* 10, 45 (2012).

18. Courbiere B, Auffan M, Rollais R *et al.*: Ultrastructural interactions and genotoxicity assay of cerium dioxide nanoparticles on mouse oocytes. *Int J Mol Sci* 14(11), 21613-21628 (2013).
19. Taylor U, Barchanski A, Petersen S *et al.*: Gold nanoparticles interfere with sperm functionality by membrane adsorption without penetration. *Nanotoxicology* 10.3109/17435390.2013.859321, (2013).
20. Barkalina N, Jones C, Coward K: Mesoporous silica nanoparticles: a potential targeted delivery vector for reproductive biology? *Nanomedicine (Lond)* 9(5), 557-560 (2014).
21. Barkalina N, Jones C, Kashir J *et al.*: Effects of mesoporous silica nanoparticles upon the function of mammalian sperm in vitro. *Nanomedicine* 10(4), 859-870 (2014).
22. Lehner R, Wang X, Marsch S, Hunziker P: Intelligent nanomaterials for medicine: Carrier platforms and targeting strategies in the context of clinical application. *Nanomedicine: Nanotechnology, Biology and Medicine* 9(6), 742-757 (2013).
23. Jones AT, Sayers EJ: Cell entry of cell penetrating peptides: tales of tails wagging dogs. *Journal of Controlled Release* 161(2), 582-591 (2012).
24. Patel LN, Zaro JL, Shen WC: Cell penetrating peptides: intracellular pathways and pharmaceutical perspectives. *Pharm Res* 24(11), 1977-1992 (2007).
25. Santra S, Yang H, Dutta D *et al.*: TAT conjugated, FITC doped silica nanoparticles for bioimaging applications. *Chem Commun (Camb)* 10.1039/b411916a(24), 2810-2811 (2004).
26. Shi NQ, Qi XR, Xiang B, Zhang Y: A survey on "Trojan Horse" peptides: Opportunities, issues and controlled entry to "Troy". *J Control Release* 10.1016/j.jconrel.2014.08.014, (2014).
27. Farkhani SM, Valizadeh A, Karami H, Mohammadi S, Sohrabi N, Badrzadeh F: Cell penetrating peptides: Efficient vectors for delivery of nanoparticles, nanocarriers, therapeutic and diagnostic molecules. *Peptides* 57(0), 78-94 (2014).
28. Rhee M, Davis P: Mechanism of uptake of C105Y, a novel cell-penetrating peptide. *J Biol Chem* 281(2), 1233-1240 (2006).
29. Jones S, Lukanowska M, Suhorutsenko J *et al.*: Intracellular translocation and differential accumulation of cell-penetrating peptides in bovine spermatozoa: evaluation of efficient delivery vectors that do not compromise human sperm motility. *Human Reproduction* 28(7), 1874-1889 (2013).
30. Hom C, Lu J, Liong M *et al.*: Mesoporous silica nanoparticles facilitate delivery of siRNA to shutdown signaling pathways in mammalian cells. *Small* 6(11), 1185-1190 (2010).
31. Pursel VG, Johnson LA: Frozen boar spermatozoa: methods of thawing pellets. *Journal of Animal Science* 42(4), 927-931 (1976).
32. Pursel VG, Rampacek GB, Johnson LA: Acrosome morphology of boar spermatozoa incubated before cold shock. *Journal of Animal Science* 34(2), 278-& (1972).
33. Burgess A, Vigneron S, Brioudes E, Labbe JC, Lorca T, Castro A: Loss of human Greatwall results in G2 arrest and multiple mitotic defects due to deregulation of the cyclin B-Cdc2/PP2A balance. *Proc Natl Acad Sci U S A* 107(28), 12564-12569 (2010).
34. Garcia-Vazquez FA, Garcia-Rosello E, Gutierrez-Adan A, Gadea J: Effect of sperm treatment on efficiency of EGFP-expressing porcine embryos produced by ICSI-SMGT. *Theriogenology* 72(4), 506-518 (2009).
35. Yamauchi Y, Riel JM, Ward MA: Paternal DNA damage resulting from various sperm treatments persists after fertilization and is similar before and after DNA replication. *J Androl* 33(2), 229-238 (2012).
36. Ben-David Makhluf S, Qasem R, Rubinstein S, Gedanken A, Breitbart H: Loading magnetic nanoparticles into sperm cells does not affect their functionality. *Langmuir* 22(23), 9480-9482 (2006).
37. Fynewever TL, Agcaoili ES, Jacobson JD, Patton WC, Chan PJ: In vitro tagging of embryos with nanoparticles. *J Assist Reprod Genet* 24(2-3), 61-65 (2007).
38. Wiwanitkit V, Sereemaspun A, Rojanathanes R: Effect of gold nanoparticles on spermatozoa: the first world report. *Fertil Steril* 91(1), E7-E8 (2009).

39. Moretti E, Terzuoli G, Renieri T *et al.*: In vitro effect of gold and silver nanoparticles on human spermatozoa. *Andrologia* 10.1111/and.12028, doi: 10.1111/and.12028. (2012).
40. Garcia-Vazquez FA, Ruiz S, Grullon LA, de Ondiz A, Gutierrez-Adan A, Gadea J: Factors affecting porcine sperm mediated gene transfer. *Res Vet Sci* 91(3), 446-453 (2011).
41. Hsieh MS, Shiao NH, Chan WH: Cytotoxic effects of CdSe quantum dots on maturation of mouse oocytes, fertilization, and fetal development. *Int J Mol Sci* 10(5), 2122-2135 (2009).
42. Huang X, Zhuang J, Teng X *et al.*: The promotion of human malignant melanoma growth by mesoporous silica nanoparticles through decreased reactive oxygen species. *Biomaterials* 31(24), 6142-6153 (2010).